

## Molecular Dynamics Study of Temperature Dependent Plastic Collapse of Carbon Nanotubes under Axial Compression

Chengyu Wei<sup>1,2</sup>, Deepak Srivastava,<sup>2</sup> and Kyeongjae Cho<sup>1</sup>

**Abstract:** The temperature dependence of the plastic collapse of single-wall carbon nanotubes under axial compression has been studied with classical molecular dynamics simulations using Tersoff-Brenner potential for C-C interactions. At zero temperature, an (8,0) single-wall carbon nanotube under axial compression collapses by forming fins-like structure which remains within the elastic limit of the system, in agreement of previous molecular dynamics study. At finite temperatures, however, we find that temperature dependent fluctuations can activate the formation of sp<sup>3</sup> bonds, in agreement with a recently proposed plastic collapse mechanism of the same nanotube with a generalized tight-binding molecular dynamics description. Furthermore, Stone-Wales defects are also found in the plastically collapsed structures. The thermal fluctuations are shown to drive nanotubes to overcome the energy barriers leading to plastically collapsed structures which have significantly lower strain energy (0.1eV/atom) than fins-like structure.

Since their discovery in 1991, [Iijima (1991), Iijima and Ichihashi (1993)] single- and multi-walled carbon nanotubes (CNTs) are shown to have exceptionally strong and stiff mechanical characteristics along the axis of the tube, and to be very flexible normal to the tube axis.[Iijima, Brabc, Maiti, Bernholc (1996); Despres, Daguerrre, Lafdi (1995); Chopra, Bebedict, Crespi, Cohen, Louse, Zettl (1995); Ruoff, Lorents (1995); Yakobson, Brabec, Bernholc (1996); Falvo, Clary, Taylor, Chi, Brooks, Washburn, Superfine (1997); Srivastava, Barnard (1997); Knechtel, Dusberg, Blau (1998); Clauss, Bergeron, Johnson (1998); Bernholc, Brabec, Buongioron, Maiti, Yakobson (1998)]

For axial deformations, the Young's modulus of single-walled CNTs can be larger than 1 TPa, and some efforts have been made to take advantage of this strength to use CNT as a reinforcing fiber in nanotube-polymer composite matrix. [Schadler, Giannaris, Ajayan (1998); Andrews, Jacques, Rao, Rantell, Derbyshire, Y. Chen, J. Chen, Haddon (1999); Ajayan, Schadler, Giannaris, Rubio (2000); Qian, Dckey, Andrews, Rantell (2000)] To develop a fully optimized nanotube composite materials, it is important to characterize the nanomechanics of CNTs.

Many experimental and theoretical efforts have been made to study CNT mechanics. [Iijima, Brabc, Maiti, Bernholc (1996); Despres, Daguerrre, Lafdi (1995); Chopra, Bebedict, Crespi, Cohen, Louse, Zettl (1995); Ruoff, Lorents (1995); Yakobson, Brabec, Bernholc (1996); Falvo, Clary, Taylor, Chi, Brooks, Washburn, Superfine (1997); Srivastava, Barnard (1997); Knechtel, Dusberg, Blau (1998); Clauss, Bergeron, Johnson (1998); Bernholc, Brabec, Buongioron, Maiti, Yakobson (1998)] The initial investigations, using classical molecular dynamics (MD) simulations with Tersoff-Brenner potential, have shown extreme stiffness of the tubes under axial compression, and the system is shown to remain in elastic limit even for very large deformations (up to 15%). [Yakobson, Brabec, Bernholc (1996); Srivastava, Barnard (1997); Bernholc, Brabec, Buongioron, Maiti, Yakobson (1998)] Non-linear elastic instabilities, with the appearance of fins-like structure, were observed in MD simulations, but the system remained within elastic limit and returned to the original unstrained state as soon as constraining forces were removed. However, more accurate generalized tight-binding (TB) MD simulations [Srivastava, Menon, Cho (1999)] have recently shown that an axial compression leads to a plastic collapse of the system that is driven by a graphitic (sp<sup>2</sup>) to diamond-like (sp<sup>3</sup>) bonding transition at the location of a collapse. At zero or low temperatures, classical MD simulations find that CNT remains within elastic limit upto

<sup>1</sup> Department of Mechanical Engineering, Stanford University, California 94305-4040

<sup>2</sup> NASA Ames Research Center, MS T27A-1, Moffett Field, California 94035-1000

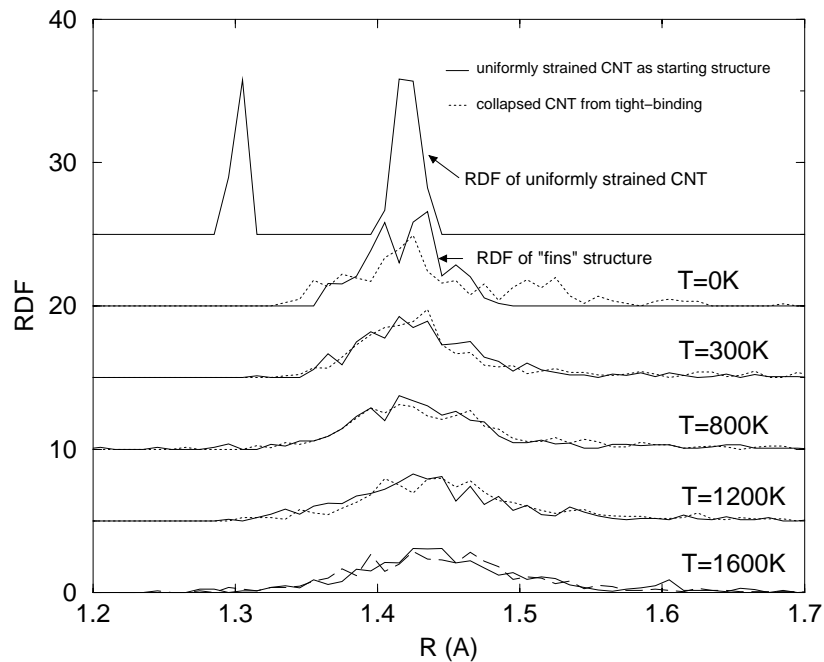


**Figure 1** : The radial distribution function (RDF) as a function of radial distance is shown for the two collapsed structures of the CNT starting from different initial configurations: one from uniformly strained CNT (solid lines), and the other from the collapsed structure of tight-binding MD simulations (dotted lines). The RDFs are similar for both simulations at 300K, 800K, 1200K and 1600K. At 0K, however, there are differences since the structure with “fins” has no sp<sup>3</sup> bond formation.

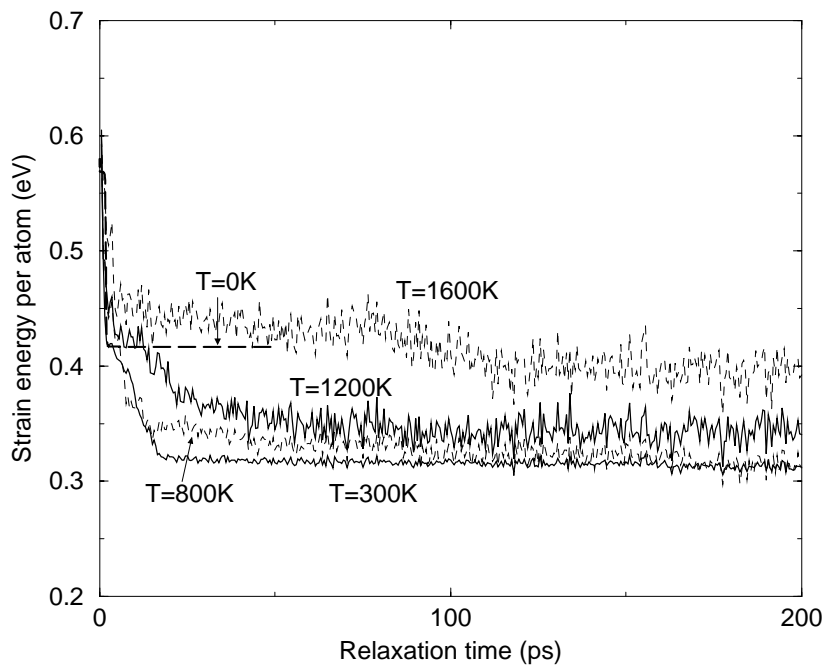


**Figure 2** : The strain energy per atom as a function of relaxation time at various temperatures. At non-zero temperatures, thermal activation induces CNT collapses to a structure with lower strain energy than the structure with “fins” (dashed line at  $T = 0K$ ).

15% strain, whereas the generalized tight-binding molecular dynamics (GTBMD) descriptions show that a crossover to plastic regimes occurs at 12% strain, through a local diamond structure formation.

The generalized tight-binding MD is considered to be more accurate in describing the energy of the system than Tersoff-Brenner potential [Tersoff (1988); Brenner (1990)] used in the classical MD studies. During the relaxation at zero temperature using Tersoff-Brenner potential, [Tersoff (1988); Brenner (1990)] only the nearest local minimum strain energy state can be reached, as there might be a barrier to the plastic collapse of the structure. In this work, we investigate how temperature dependent fluctuations might help in overcoming this structural energy barrier and give a plastically collapsed structure that is similar to that obtained with the generalized tight-binding molecular dynamics method.

An (8,0) CNT was chosen for the temperature dependent simulations to keep the CNT system same as that was studied with the tight-binding molecular dynamics method at zero temperature. Also for a direct comparison with the tight-binding MD simulation results, we start with a 12% uniformly compressed section of the tube (that is about 40 Å long) since tight-binding MD finds the (8,0) CNT begins to plastically collapse at such strain. Keeping the both ends of the tube fixed at the strained values and letting the CNT relax using classical MD with Tersoff-Brenner potential at zero temperature, we find, not surprisingly, that the CNT does not stay in the uniform structure, and that “fins” structure appears to relieve some of the strain energy in the system. The radial distribution function (RDF) of the nanotube before elastic collapse (Fig.1) shows a peak at about 1.3 Å which disappears after “fins” structure appears. The peaks representing the bond lengths are distributed between 1.35 to 1.5 Å. Although “fins” structure reduces the strain energy, the deformation is fully elastic as was found also in previous studies. After removing the strains at the ends of the tube, the CNT recovers to its initial unstrained structure, and no sp<sup>3</sup> bonds were observed at any stage within the structural configuration of the “fins.”

To overcome possible energy barrier and explore larger region of the configuration space, we performed finite temperature classical MD simulations of the strained CNT section. The uniformly compressed CNT in the above example was dynamically relaxed, for durations much longer than the relaxation times, at temperatures

of 300K, 800K, 1200K and 1600K, respectively. Fig. 2 shows the changes in the strain energy as a function of the relaxation time. It is observed that the finite temperatures do help CNT to relax to energetically favorable structures. The zero temperature strain energy of the CNT with “fins” like structure is also plotted. At T=300K and T=800K, the strain energy per atom becomes lower than the energy of the CNT with “fins” structure after 10ps relaxation. The strain energy of the finally relaxed structure as a function of temperature is shown as a continuous line in Fig. 3. We can see that at T=300K and T=800K, the strain energy is lowered further by about 0.1eV/atom below the energy of the structure with “fins”. At higher temperatures, T=1200K and T=1600K, the higher total strain energy of the system is observed due to larger vibrational contributions to the total potential energy of the system.

The configurations of relaxed CNTs at various temperatures are shown in Fig. 4 along with the zero temperature structure with “fins.” A collapsed region appears in the CNT at finite temperature. To check if the collapsed structure is due to plastic deformation, we track the appearance of sp<sup>3</sup> bond formation during the dynamics of the relaxation at finite temperatures. Fig. 5 shows the average of the number of carbon atoms which have four nearest neighbors (sign of the formation of sp<sup>3</sup> bond) as a function of the relaxation time. In Fig. 5 we can see that at T=300K, sp<sup>3</sup> bond begins to appear after about 1ps. At T=800K, the sp<sup>3</sup> bonds form after 0.5ps of MD simulation. At higher temperatures, T=1200K and T=1600K, the sp<sup>3</sup> bond begins to appear even at shorter relaxation times, and this indicates a thermal activation barrier to form sp<sup>3</sup> bond. The plastic nature of the deformations was tested by removing the strain constraints at the ends of the relaxed CNT, and dynamically further relaxing the system. The CNT did not relax back to the starting unstrained configuration, and irreversible nature of the collapse has been confirmed.

In the tight-binding MD simulations, [Srivastava, Menon, Cho (1999)] the CNT was found to collapse at 12% compression strain. To test the stability of final structures with the thermally activated collapse, the collapsed structure from the tight-binding MD simulation was used as initial configuration of classical MD simulations at several temperatures. A comparison of the radial distribution functions (RDFs) of both collapsed structures is shown in Fig. 1.

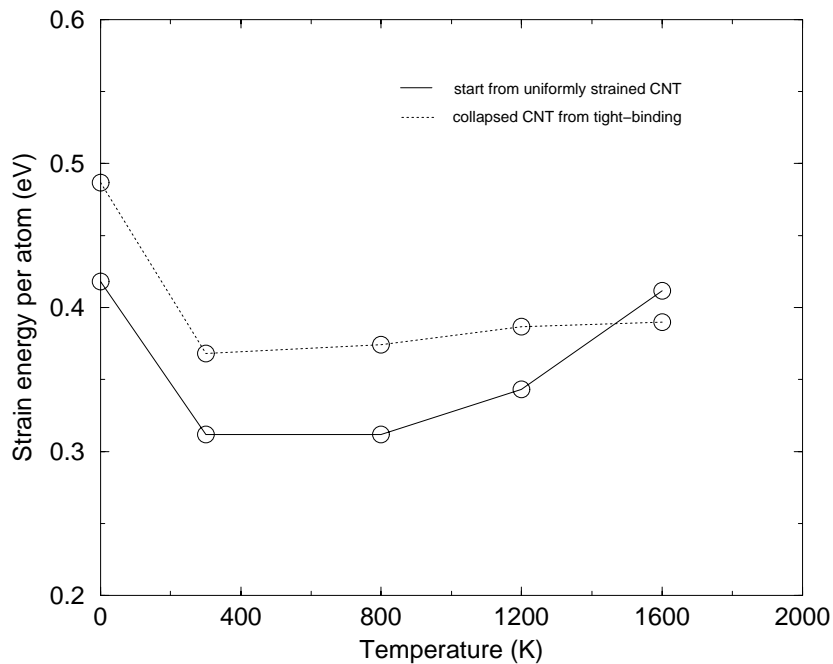


**Figure 3** : The strain energy per atom as a function of temperature. The solid line is for the structure relaxed from uniformly strained CNT using classical MD simulations. The dotted line is for structure relaxed using MD starting from a collapsed CNT from tight-binding MD simulations. The two collapsed structures have similar strain energies at higher temperature (1200K and 1600K).

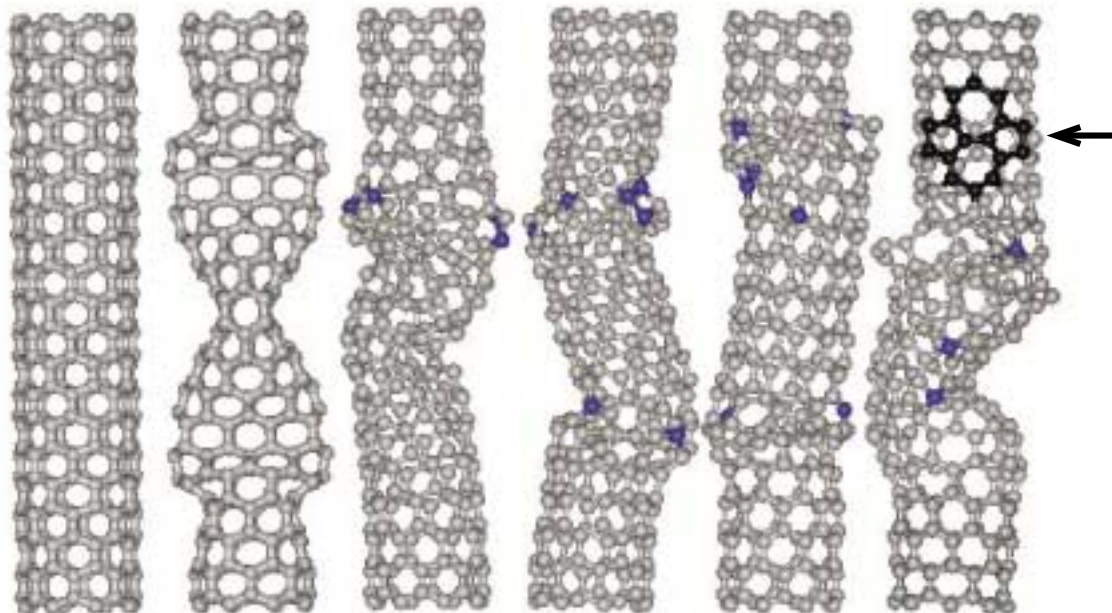


**Figure 4** : The configurations of a 12% strained (8,0) CNT relaxed at different temperatures are shown. The first configuration is a uniformly strained CNT. The “fins” like deformations occur and are shown in the second structure at 0K. The third to sixth structures correspond to simulations at 300K, 800K, 1200K, 1600K, respectively. At finite temperatures, some sections of CNT have collapsed with  $sp^3$  bond formation, and also with formation of Stone-Wales defect. One such defect is indicated by an arrow in the sixth structure.

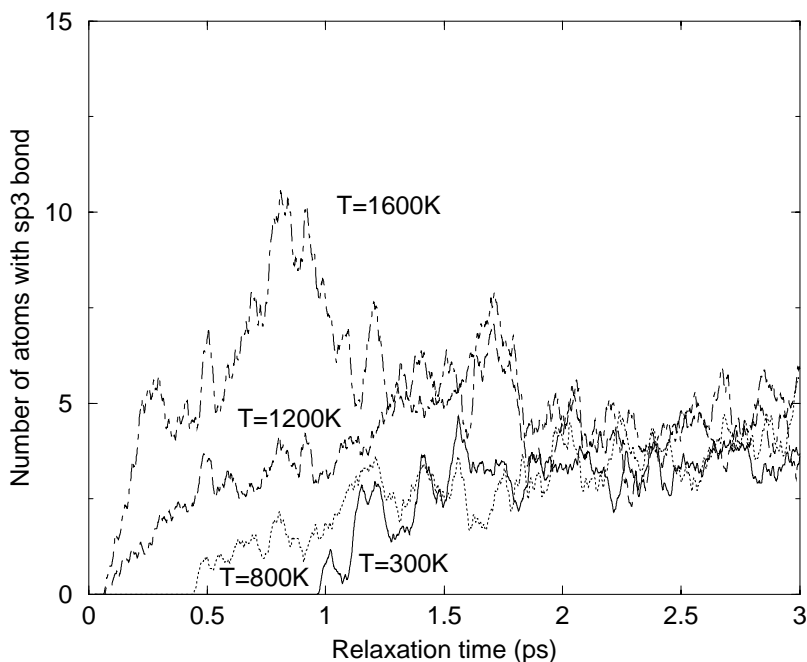


**Figure 5** : The average number of atoms with sp3 bonds as a function of relaxation time at different temperatures are shown. Higher temperatures activate the formation of sp3 bond at earlier time.

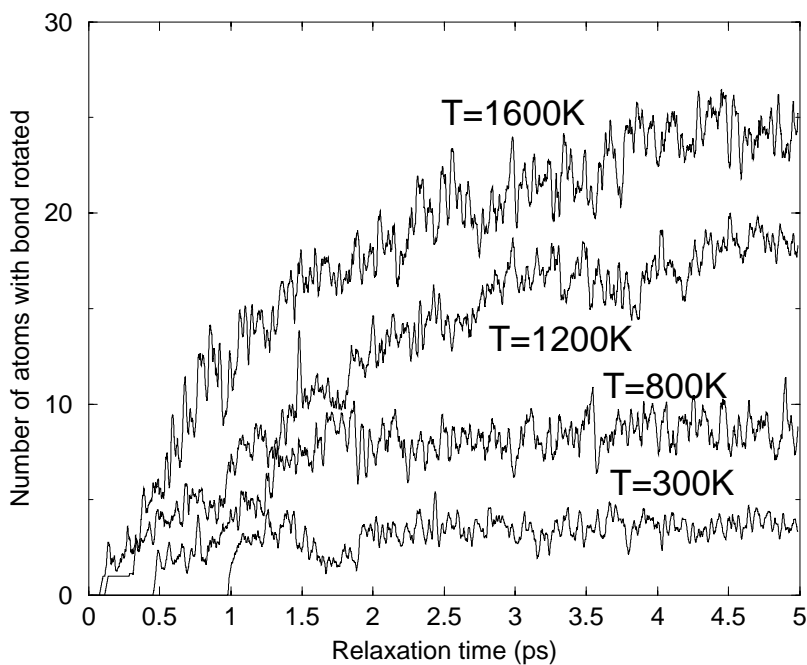


**Figure 6** : The average number of atoms participating in bond rotation induced defects as a function of relaxation time are plotted at different temperatures. Higher temperatures activate bond rotations earlier time.

At zero temperature, there is a wide distribution of the peaks from 1.4 Å to 1.7 Å suggesting formation of some sp<sup>3</sup> bonds (peak at 1.5 Å), which is different from the RDF of the structure with “fins”, where no distribution beyond 1.5 Å is observed. At non-zero temperatures, we find that the two collapsed structures show similar RDF patterns, where both have wide distribution extending upto to 1.7 Å. The comparison of the strain energy in the two cases (in Fig.3) show that the thermally activated collapsed structures from classical MD simulations have lower strain energy than the collapsed structures starting from the tight-binding MD simulations. We believe that this difference comes from the details of the parameterization in Tersoff-Brenner potential leading to different relative energies. Furthermore, the energy barriers between the elastically strained structure of CNT and the collapsed ones in our classical MD simulations can be estimated from the relaxation time  $t = t_0 \exp(E_\gamma/KT)$ . For C-C bond the characteristic time of vibration is about 0.1ps, and the barrier  $E_\gamma$  is estimated to vary from 0.15 eV to 0.9 eV.

Besides sp<sup>3</sup> bond formation, “Stone-Wales” dislocations are also observed in our simulations at high temperature. As shown in Fig. 4, for T=1600K, two “Stone-Wales” dislocations can be seen back to back at the upper section of the compressed CNT. Such bond rotations are found on CNTs in large tensile stress by classical MD simulations at high temperatures, [Nardelli, Yakobson, Bernholc (1998)] but for compression, such defects were not seen by Tight-Binding MD simulations which were conducted at T=0K. In Fig. 6, the number of atoms with bond rotation induced defects is plotted as function of relaxation time up to 5ps. Similar to the formations of the sp<sup>3</sup> bonds, we find that at higher temperatures bond rotations occur more frequently.

In summary, we have used classical MD with Tersoff-Brenner potentials to simulate the collapse of CNT at finite temperatures. This is different from the previous classical MD study. We find that at non-zero temperatures, in the range 300-1600K, classical MD with Tersoff-Brenner potential also causes the structure of CNT to collapse locally with the formation of diamond like bonds at the location of the collapse. The role of non-zero temperature is to help overcome the energy barrier that exist between the previously found “fins” like structure and the locally collapsed structures observed in the tight-binding MD simulations. The Stone-Wales dislocations are also found at high temperature. The thermally

activated collapse is found to be plastic in nature in agreement with the tight-binding MD simulation predictions and experimental observations.

**Acknowledgement:** This project is supported by a grant from NASA

## References

- Iijima, S.** (1991): Helical microtubules of graphitic carbon. *Nature*, vol. 354, pp. 56-58.
- Iijima, S. and Ichihashi, T.** (1993): Single-shell carbon nanotubes of 1-nm diameter. *Nature*, vol. 363, pp. 603-605.
- Bethune, D.S.; Kiang, C.-H.; deVries, M.S.; Gorman, G.; Savoy, R.; Vazquez, J.; and Beyers R.** (1993): Cobalt-catalyzed growth of carbon nanotubes with single-atomic-layer walls. *Nature*, vol. 363, pp. 605-607.
- Iijima, S.; Brabec, C.; Maiti, A.; and Bernholc, J.** (1996): Structural flexibility of carbon nanotubes. *J. Chem. Phys.*, vol. 104, pp. 2089-2092.
- Despres, J.; Daguerre, E.; and Lafdi, K.** (1995): Flexibility of graphite layers in carbon nanotubes. *Carbon*, vol. 33, pp. 87-89.
- Chopra, N.; Bebedict, L.; Crespi, V.; Cohen, M.L.; Louie, S.G.; and Zettl, A.** (1995): Fully collapsed carbon nanotubes. *Nature*, vol. 37, pp. 135-138.
- Ruoff, R. and Lorents, D.** (1995): Mechanical properties of carbon nanotube. *Bull. Am. Phys. Soc.*, vol. 40, pp. 173.
- Yakobson, B.I.; Brabec, C.J.; and Bernholc, J.** (1996): Nanomechanics of carbon tubes: Instabilities beyond linear response. *Phys. Rev. Lett.*, vol. 76, pp. 2511-2514.
- Falvo, M.R.; Clary, G.J.; Taylor II, R.M.; Chi, V.; Brooks, F.P. Jr.; Washburn, S.; and Superfine, R.** (1997): Bending and buckling of carbon nanotubes under large strain. *Nature*, vol. 389, pp. 582-584.
- Srivastava, D. and Barnard, S.** (1997): Molecular dynamics simulation of large-scale carbon nanotubes on a shared-memory architecture. *Proceedings of IEEE Supercomputing '97 (SC '97)*, CDROM version.
- Knechtel, W.H.; Dusberg, G.S.; and Blau, W.J.** (1998): Reversible bending of carbon nanotubes using a transmission electron microscope. *Appl. Phys. Lett.*, vol. 73, pp. 1961-1963.

**Clauss, W.; Bergeron, D.J.; and Johnson, A.T.** (1998): Atomic resolution STM imaging of a twisted single-wall carbon nanotube. *Phys. Rev. B*, vol. 58, pp. 4266-4269.

**Bernholc, J.; Brabec, C.; Buongioron, M.; Maiti, A.; Yakobson, B.I.** (1998): Theory of growth and mechanical properties of nanotubes. *Appl. Phys. A*, vol. 67, pp. 39-46.

**Schadler, L.S.; Giannaris, S.C.; and Ajayan, P.M.** (1998): Load transfer in carbon nanotube epoxy composites. *Appl. Phys. Lett.*, vol. 73, pp. 3842-3844.

**Andrews, R.; Jacques, D.; Rao, A.M.; Rantell, T.; Derbyshire, F.; Chen, Y.; Chen, J.; and Haddon, R.C.** (1999): Nanotube composite carbon fibers. *Appl. Phys. Lett.*, vol.75, pp. 1329-1331.

**Ajayan, P.M.; Schadler, L.S.; Giannaris, C.; and Rubio, A.** (2000): Single-walled carbon nanotube-polymer composites: Strength and weakness. *Advanced Materials*, vol. 12, pp. 750.

**Qian, D.; Dickey, E.C.; Andrews, R.; and Rantell, T.** (2000): Load transfer and deformation mechanisms in carbon nanotube-polystyrene composites. *Appl. Phys. Lett.*, vol. 76, pp. 2868-2870.

**Srivastava, D.; Menon, M.; and Cho, K.** (1999): Nanoplasticity of single-wall carbon nanotubes under uniaxial compression. *Phys. Rev. Lett.*, vol. 83, pp. 2973-2976.

**Tersoff, J.** (1988): New empirical-approach for the structure and energy of covalent systems. *Phys. Rev. B*, vol. 37, pp. 6991-7000.

**Brenner, D.W.** (1990): Empirical potential for hydrocarbons for use in simulating the chemical vapor-deposition of diamond films. *Phys. Rev. B*, vol. 42, pp. 9458-9471.

**Nardelli, M.B.; Yakobson, B.I.; and Bernholc J.** (1998): Brittle and ductile behavior in carbon nanotubes. *Phys. Rev. Lett.*, vol. 81, pp. 4656-4659.

